IN-FLIGHT FAR-INFARED PERFORMANCE OF THE CIRS INSTRUMENT ON CASSINI

Conor A. Nixon[1], John C. Brasunas[2], Brook Lakew[2], Rainer Fettig[3], Donald E. Jennings[2], Ronald Carlson[4], Virgil G. Kunde[1]

[1] Department of Astronomy, University of Maryland, College Park, MD 20742
[2] NASA Goddard Space Flight Center, Code 693, Greenbelt, MD 20771
[3] Institute fur Mikrostrukturtechnik, Karlsruhe, Germany
[4] S. S. A. I., 10210 Greenbelt Road, Suite 600, Lanham, MD 20706

ABSTRACT

The Composite Infrared Spectrometer (CIRS) on-board Cassini consists of two interferometers: a conventional Michelson for the mid-infrared; and a Martin-Puplett type in the far-infrared employing wire grid polarizers to split, recombine and analyze the radiation. The far-IR focal plane (FP1) assembly uses two thermopile detectors to measure the final transmitted and reflected beams at the polarizer-analyzer: if one fails, the interferometer can still operate, albeit with a lower efficiency. The combined effect is for good response from 10 to 300 cm^{-1}, and declining response to 600 cm^{-1}. This paper will examine in-flight performance of the far-IR interferometer, including NESR and response. Regular noise spikes, resulting from pickup from other electrical sub-systems has been found on the CIRS interferograms, and the removal of these effects is discussed. The radiometric calibration is described, and then we show how the calibration was applied to science data taken during the Jupiter flyby of December 2000. Finally, we discuss signal-to-noise on the calibrated spectra, emphasizing limitations of the current instrument and the potential for improvement in future missions.

INTRODUCTION

The CIRS instrument carried on-board the Cassini spacecraft mission to Saturn is the conceptual successor to the highly successful IRIS (Infrared Interferometer Spectrometer) instrument which flew on both Voyager spacecraft, although improved in almost every respect. CIRS was conceived and built by an international team including institutions in the USA, UK, France and Germany, and led by NASA Goddard Space Flight Center.

CIRS is a dual interferometer, and has been previously described in the literature[1, 2]. The Michelson mid-infrared interferometer and the Martin-Puplett type far-infrared interferometer both share a common mirror scan mechanism, reference laser and telescope assembly, although the beamsplitters and detectors are quite different. The telescope consists of a 50 cm F/6 paraboloidal primary mirror and 7.6 cm diameter hyperboloidal secondary mirror, both of beryllium. A field splitting mirror divides the radiation into the two interferometers. The far-IR radiation then passes through a solar-blocking filter, collimator and folding flat before reaching the polarizing beam splitter. The solar blocker rejects rays short-ward of 16.7 microns.
The input polarizer, beamsplitter and output analyzer are each 1 micron diameter photolithographic copper wires with a spacing of 2 micron, deposited on mylar. These give near 100% efficiency from 10 to 300 cm^{-1}, and good though declining efficiency from 300 to 600 cm^{-1}, the limit of the nominal range.

PRE-PROCESSING OF RAW INTERFEROGRAMS

CIRS interferograms (IFMs) suffer from several distinct types of noise interference. Firstly, there is a sine wave ripple on the IFM baseline, which was seen intermittently between launch and Jupiter flyby, with varying period and amplitude. Because of its transient nature, it has not been well characterized, although during the science phase of the Jupiter flyby its amplitude had diminished so that it did not significantly affect performance.

[1] *Contact information for C.A. Nixon- Email: conor.nixon@gsfc.nasa.gov*

The second and third types are repetitive sequences of sharp spikes, or delta functions, which appear as a 'comb' on the IFMs. These have periods (frequencies) of 0.125 seconds (8 Hz) and 2.0 seconds (0.5 Hz) respectively. Both are caused by the CIRS Bus Interface Unit (BIU), which is queried 8 times a second by the spacecraft Command Data Subsystem (CDS), on the spacecraft clock signal pulses. Each query causes a small spike. Then, every 2 seconds data is transferred from CIRS to the CDS, which causes a larger spike.

Only the 0.5 Hz BIU interface spikes are large enough and repeatable enough to be treated by algorithmic methods at the present time. Fig. 1 ('before') shows a typical far-IR IFM before spike removal. CIRS IFMs are partially double-sided, consisting of a short scan at negative path difference and then a much longer scan at positive path difference after the zero path difference (ZPD) point, at sample 90. The first step in spike removal is to create a spike comb (shown offset above the IFM) having the correct period. This comb is then cross-correlated with the IFM to determine the best-fitting absolute offset.

Spikes may sometimes be offset by +/- 1 sample from the expected position, due to the discretization process. To correct for this, a statistical technique is also used to hunt for spikes, defined as noise peaks above 2.5-σ in amplitude. If a 2.5-σ peak occurs immediately before or after a predicted spike position, then the comb spike is moved. Statistically detected positions are labeled below the IFM on Fig. 1.

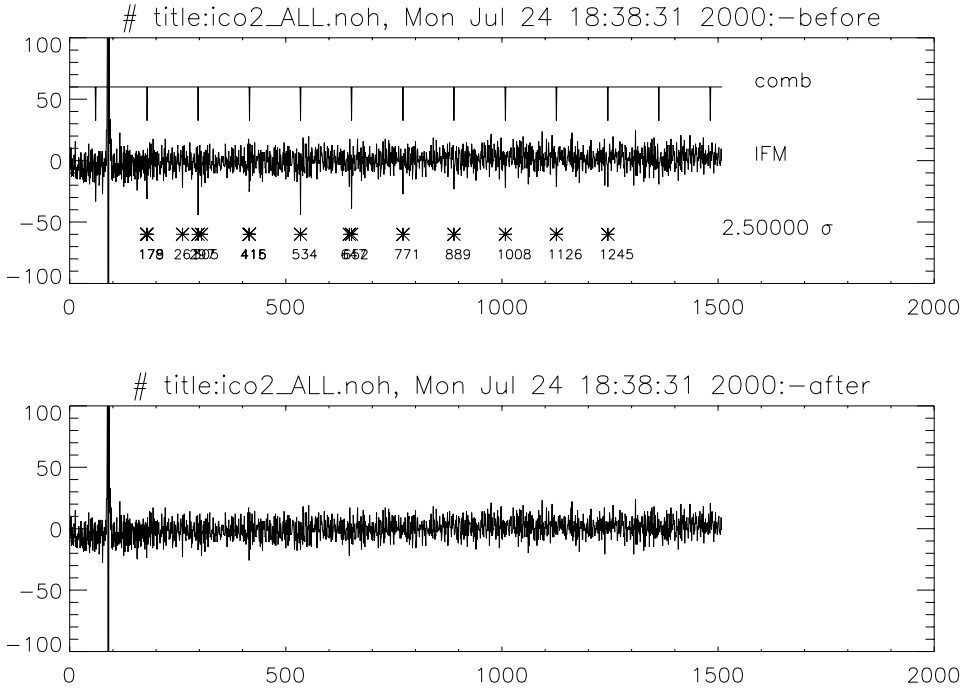

Figure 1: *Example of removal of interference spikes by comb technique.*

Finally, the comb amplitude is scaled to the mean value of the IFM at the predicted positions. The resulting comb is the best-guess model of the 0.5 Hz spike pattern inherent in the data. This comb is subtracted from the IFM, resulting in a 'cleaned' or 'noise-filtered' IFM, as shown in Fig. 1 ('after'). Clearly, much of the regular spike pattern has been removed.

RADIANCE CALIBRATION

The most important calibration task concerns the absolute radiance, expressed by the spectral responsivity. In-flight calibration of the responsivity traditionally has been achieved by exposing the instrument to two well-known calibration sources. One is usually deep space, which for this purpose is assumed to be a perfect sink. The second source is often a blackbody of accurately known temperature. Perfect linearity and thermal stability of the instrument are required. An alternate approach, which was well demonstrated on Voyager, is to thermostat the

instrument, the primary and the secondary mirror of the telescope at the same low temperature. Again, one calibration source is deep space while the other is replaced by a virtual blackbody at the instrument temperature. This method of calibration is directly applicable to the far infrared interferometer since all elements, including the detector, are precisely at the same temperature.

The spectral responsivity in the far-IR is simply the complex FFT power spectrum when looking at deep space, divided by the difference in Planck function radiance between space and the instrument (170 K):

$$r(\nu) = \frac{FFT(I_{cold})}{B_{cold}(\nu) - B_{instr}(\nu)} \quad \ldots (1)$$

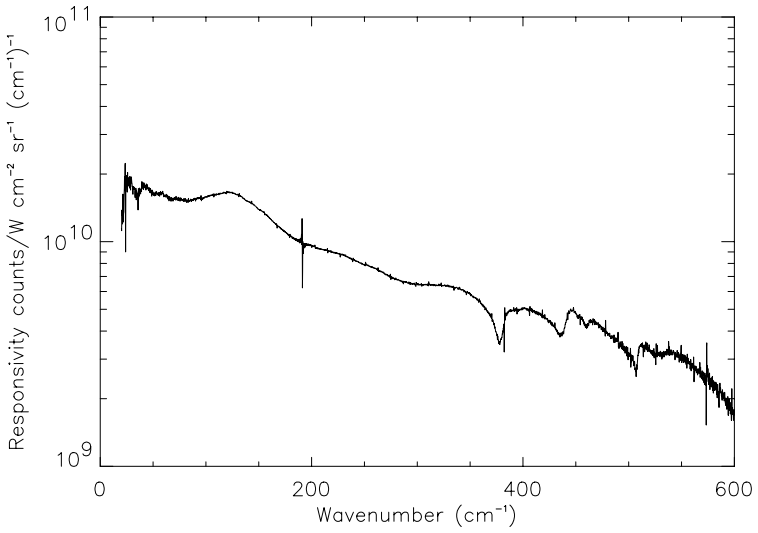

Figure 2: *CIRS spectral responsivity.*

Fig. 2 shows the CIRS responsivity in the far-IR. There are several important features. Firstly, the response declines by 1 order of magnitude from 20 cm^{-1} to 600 cm^{-1}, as a combination of effects from the various optical elements, coatings and detectors; mainly the wire grid polarizer/analyzers, but also the digital filter beyond 500 cm^{-1}. Secondly, the deep, broad absorption features seen at 380, 440 and 510 cm^{-1} arise from the mylar substrate on which the grids are deposited. Thirdly, the most prominent narrow features arise from the 8 Hz interference (191 cm^{-1}), along with its harmonics at 16 Hz (382 cm^{-1}) and 24 Hz (573 cm^{-1}). Finally, the pattern of smaller sharp lines above and below the continuum which become noticeable after 400 cm^{-1} result from the 0.5 Hz interference, having a spacing of 11.9 cm^{-1}.

The responsivity, once determined, is used to calibrate science ('target') IFM scans as follows:

$$B_{t\,\mathrm{arg}} = B_{cold} - \frac{FFT(I_{t\,\mathrm{arg}} - I_{cold})}{r(\nu)} \quad \ldots (2)$$

EARLY RESULTS FROM JUPITER FLYBY

Fig. 3 shows a typical CIRS far-IR spectrum of Jupiter at 0.5 cm^{-1} resolution. 100 spectra (each a 50-second scan) from January 2001 have been co-added to reduce random noise and emphasize features in the data. The very broad absorption feature from 250-500 cm^{-1} is the S(0) collisionally-induced continuum of H_2; part of the S(1) absorption is visible from 500-600 cm^{-1}. To show other absorptions more clearly, a 25 cm^{-1} smoothing kernel was applied to the data to create a rough continuum fit, which was then subtracted from the spectrum. The result is plotted as the discontinuous line in the middle of the figure, which shows the molecular absorption features more clearly.

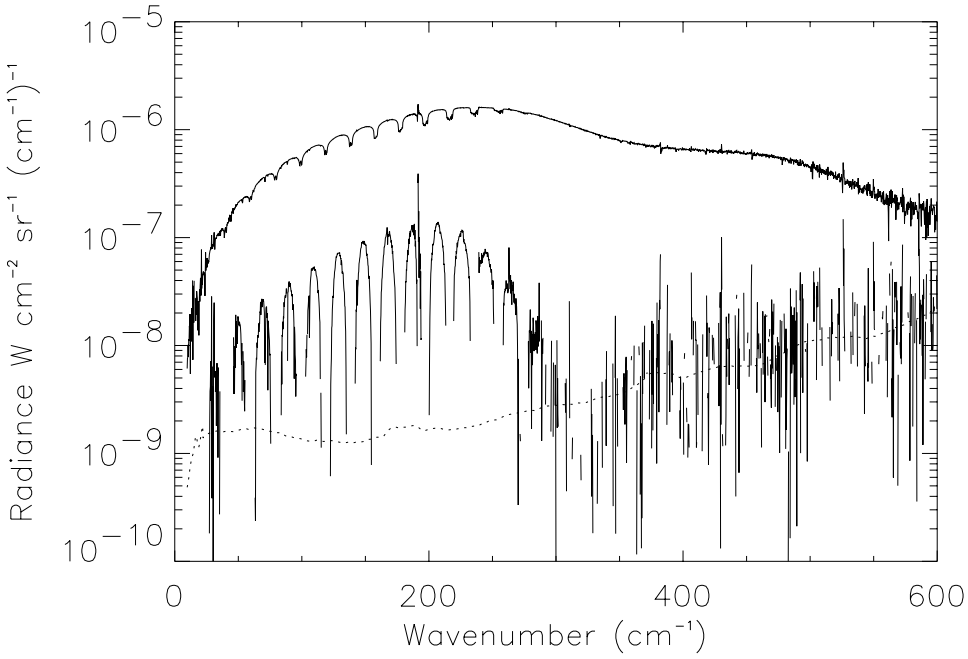

Figure 3: *Far-infrared spectrum, and noise comparison.*

For comparison, the 100-spectrum smoothed NESR is also plotted (dotted line). The NESR is the limit of detection of weak features. Clearly, the NH_3 and PH_3 absorption features (20-250 cm^{-1}) are well above the noise level. CIRS has also detected pure rotational lines of CH_4 in the 70-120 cm^{-1} region, for the first time on Jupiter. However, beyond 350 cm^{-1} the difference spectrum is equivalent to the noise, and no features are seen in this average. Co-adding up to 1300 spectra has enabled detections of HD lines at 89 and 265 cm^{-1}, at S/N of 8 to 10. Other HD and H_2 features are either masked by stronger bands or mingled with noise interference. Finally, ISO has seen emission lines of water [3] at 100-250 cm^{-1}, which are below the threshold of sensitivity achieved thus far with CIRS.

CONCLUSIONS

At Jupiter CIRS demonstrated that it will meet the requirements of the Cassini IR investigation and will achieve the science goals of its prime mission at Saturn. In the future, improvements in sensitivity for this type of far-IR FTS instrument will become possible with technology currently under development. These will be valuable in reducing the observation times (co-adding) required to detect weak lines in the 10–600 cm^{-1} spectral region on Jupiter and the other giant planets. Smaller averages will enable spatial mapping of D/H and gaseous abundances in the same time as present global detections. Greater sensitivity will arise from improvements in technology of the thermal detectors, and also optical components such as far-IR beamsplitters. We recommend that future instruments, before launch, carefully look for and eliminate the type of system-related interferences seen by CIRS, which add to the difficulty of reducing data.

REFERENCES

1. V. Kunde *et al., Cassini Infrared Fourier Spectroscopic Investigation,* Proc. of Cassini/Huygens: A Mission to the Saturnian System, SPIE Proceedings, Vol. 2803, p162, 1996.
2. J.C. Brasunas and B. Lakew, *Long-term stability of the Cassini Fourier transform spectrometer en route to Saturn,* Recent Research Developments in Optics, Research Signpost, Kerala, India, 2003.
3. E. Lellouch et al., *The Origin of Water Vapor and Carbon Dioxide in Jupiter's Stratosphere,* Icarus, Vol. 159, p112, 2002.